Tuning the thickness of exfoliated quasi-two-dimensional β–Ga_2O_3 flakes by plasma etching

Yongbeom Kwon, Geonyeop Lee, Sooyeoun Oh, Jihyun Kim, Stephen J. Pearton, and Fan Ren

Citation: Appl. Phys. Lett. **110**, 131901 (2017); doi: 10.1063/1.4979028
View online: http://dx.doi.org/10.1063/1.4979028
View Table of Contents: http://aip.scitation.org/toc/apl/110/13
Published by the American Institute of Physics

Tuning the thickness of exfoliated quasi-two-dimensional β-Ga_2O_3 flakes by plasma etching

Yongbeom Kwon,[1] Geonyeop Lee,[1] Sooyeoun Oh,[1] Jihyun Kim,[1,a)] Stephen J. Pearton,[2] and Fan Ren[3]
[1]*Department of Chemical and Biological Engineering, Korea University, Seoul 02841, South Korea*
[2]*Department of Materials Science and Engineering, University of Florida, Gainesville, Florida 32611, USA*
[3]*Department of Chemical Engineering, University of Florida, Gainesville, Florida 32611, USA*

(Received 1 February 2017; accepted 2 March 2017; published online 27 March 2017)

We demonstrated the thinning of exfoliated quasi-two-dimensional β-Ga_2O_3 flakes by using a reactive ion etching technique. Mechanical exfoliation of the bulk β-Ga_2O_3 by using an adhesive tape was followed by plasma etching to tune its thickness. Since β-Ga_2O_3 is not a van der Waals material, it is challenging to obtain ultra-thin flakes below a thickness of 100 nm. In this study, an etch rate of approximately 16 nm/min was achieved at a power of 200 W with a flow of 50 sccm of SF_6, and under these conditions, thinning of β-Ga_2O_3 flakes from 300 nm down to ~60 nm was achieved with smooth morphology. We believe that the reaction between SF_6 and Ga_2O_3 results in oxygen and volatile oxygen fluoride compounds, and non-volatile compounds such as GaF_X that can be removed by ion bombardment. The opto-electrical properties were also characterized by fabricating solar-blind photodetectors using the plasma-thinned β-Ga_2O_3 flakes; these detectors showed fast response and decay with excellent responsivity and selectivity. Our results pave the way for tuning the thickness of two-dimensional materials by using this scalable, industry-compatible dry etching technique. *Published by AIP Publishing.* [http://dx.doi.org/10.1063/1.4979028]

One of the most promising emerging wide bandgap materials, β-Ga_2O_3, has a direct energy bandgap of ~4.9 eV at room temperature.[1] It has higher values of breakdown field and Baliga's figure of merit (BFOM) than other wide bandgap materials.[2,3] These properties make β-Ga_2O_3 attractive for next-generation high power electronic devices especially in harsh environments.[4] In addition, β-Ga_2O_3, which can detect photons in the deep ultra-violet (UV) spectral region, could be utilized for flame monitoring, detection of missiles, and UV dosimetry.[5,6] To date, crystalline β-Ga_2O_3 substrates have been obtained by various growth methods.[7–11] Film deposition of β-Ga_2O_3 has also been investigated,[1,12–15] where to this point, the crystallinity of the deposited thin-films has generally been inferior to the bulk substrates. Recently, the mechanical exfoliation method to obtain two-dimensional (2D) β-Ga_2O_3 flakes from the crystalline bulk substrate has been developed,[16–18] which allows the investigation of the (opto)electronic properties of high quality 2D β-Ga_2O_3. Mitdank *et al.*[19] reported that the properties of exfoliated crystalline films are comparable to those of the bulk single crystals. Opto-electronic devices based on the exfoliated 2D β-Ga_2O_3 have been demonstrated by fabricating a field-effect transistor (FET)[17] and a photoconductive-type solar-blind photodetector.[20] Also, the effects of the contact metal on the exfoliated β-Ga_2O_3 flakes have been characterized using different metals, ambient and annealing temperatures.[21]

Mechanical exfoliation by using an adhesive tape is a well-known technique to obtain 2D materials, of which the height can be as thin as a monolayer. Just as in the production of graphene from bulk graphite,[22] 2D flakes with high crystalline quality are separated, and they can be transferred onto any desired substrate using this method, without the lattice mismatch and growth-induced strain. However, when using this mechanical exfoliation technique, it is difficult to control the thickness of the transferred flakes,[17,20] which limits the implementation of the 2D materials into practical uses. For example, the threshold voltage of the 2D material-based FETs will depend on their thickness as the channel layer. Fine-tuning of their thickness is critical to facilitate the investigation of the electrical and opto-electronic properties of 2D materials. Lee *et al.*[23] showed that the electrical properties of 2D black phosphorus can be controlled by reducing its thickness using plasma etching. Especially in case of β-Ga_2O_3, it is challenging to obtain ultrathin flakes below a thickness of 100 nm because β-Ga_2O_3 is a three-dimensional material, not a van der Waals material. Although few-layer β-Ga_2O_3 flakes were obtained by the mechanical exfoliation technique,[16] the yield will be very low, and the size of the flakes will be small after a repeated number of the exfoliation cycles.

To control the thickness of a semiconductor, etching, either dry or wet, is commonly used. Dry etching is fast, easy to control, and highly anisotropic. Accordingly, in this paper, we report thinning of β-Ga_2O_3 flakes using a dry etching technique that has good uniformity and is suitable for large scale production. There have been few studies on etching of β-Ga_2O_3.[24–26] In the present study, we obtained the initial β-Ga_2O_3 flakes by using a mechanical exfoliation method and controlled the thickness of the flakes with the reactive ion etching (RIE) technique, which is compatible with the standard Si-based industry practices. SF_6 gas is a common etch gas in the silicon industry and is less toxic and less corrosive than chlorine or bromine. We carried out etching by using SF_6 gas and systematically analyzed the optical,

a)Author to whom correspondence should be addressed. Electronic mail: hyunhyun7@korea.ac.kr

structural, morphological, and opto-electronic properties of the plasma-etched β-Ga_2O_3 flakes.

Figure 1(a) depicts the mechanical exfoliation process of β-Ga_2O_3 from a bulk substrate (Tamura Corp.) that had been grown by the edge-defined film-fed growth method and then was transferred onto a sapphire substrate. The sample was plasma-etched using the RIE (RIE 5000, SNTEK) etcher as shown in Fig. 1(b). For the etching process, SF_6 gas with a flow rate of 50 sccm and 100–200 W of applied 13.56 MHz power at a pressure of 3.5×10^{-2} Torr was used. The etching time was varied from 5 to 15 min; and three samples were used for each etching experiment.

The surface morphology was characterized by an optical microscope (BX51M, Olympus) and a scanning electron microscope (SEM; FESEM S-4700, Hitachi). An atomic force microscope (AFM; Innova, Bruker) and a surface profiler (D-100, KLA-Tencor) were used to measure the height of the flake before and after dry etching. Note that the sapphire substrate was also etched under our RIE conditions.[27] Therefore, the height of β-Ga_2O_3 thinned by RIE was obtained by subtracting the height of the etched sapphire from the total etched height of sapphire and β-Ga_2O_3. To analyze the structural changes induced by plasma etch, transmission electron microscopy (TEM; JEM 2100 F) in conjunction with the focused-ion beam method and micro-Raman spectroscopy under back-scattering geometry using an excitation wavelength of a 532 nm diode-pumped solid-state laser was used.

For the characterization of the opto-electronic properties, two metal electrodes were defined via a standard photolithography process. The electrical properties of β-Ga_2O_3 were obtained using a semiconductor parameter analyzer (Agilent 4155 C) under a low vacuum condition (8 mTorr) at room temperature. UV illuminations at the wavelengths of 254 and 365 nm (UV lamp, UVITEC) and visible light illumination at 532 nm were chosen to obtain the spectral photoresponse properties. A time-dependent measurement of the photoresponse was carried out at 10 V under the low vacuum condition.

Figures 2(a) and 2(b) show the optical microscopic images of the β-Ga_2O_3 flake before and after the plasma etch using SF_6 gas with a flow of 50 sccm at a power of 200 W for 15 min. The residue of the adhesive tape that occurred during the dry transfer process was removed after RIE etching, which shows that plasma etching process also can be used for the removal of the transfer residues. By comparing optical microscopic images and AFM images (Figs. 2(a)–2(d)), a reduction in the width of the flake is noticeable. This is because the edges of the flake have many dangling bonds that

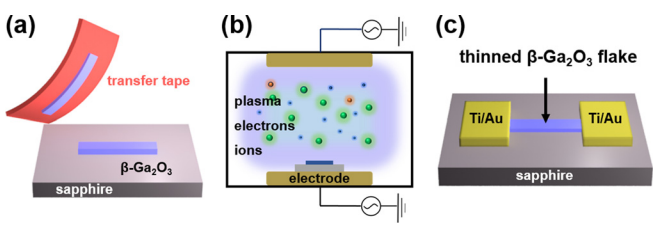

FIG. 1. Schematics of (a) mechanical exfoliation of β-Ga_2O_3, followed by dry transfer onto the sapphire substrate; (b) RIE-assisted thinning of a β-Ga_2O_3 flake; and (c) the fabricated solar-blind photodetector device using the thinned β-Ga_2O_3 flake.

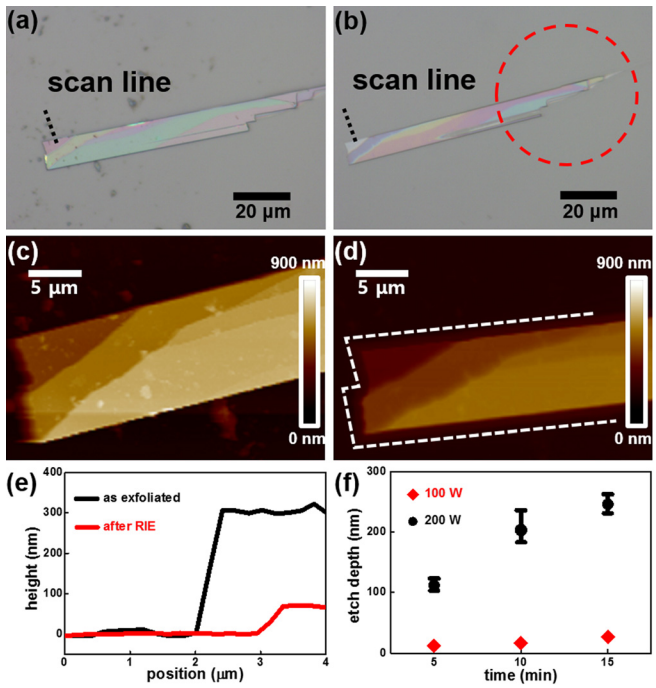

FIG. 2. Optical microscope images of an exfoliated β-Ga_2O_3 flake (a) before and (b) after plasma etching. AFM images of a β-Ga_2O_3 flake (c) before and (d) after plasma etching. (e) Height profiles of a β-Ga_2O_3 flake before (black) and after (red) plasma etching and (f) etch depth as a function of power and etching time.

can readily react with the fluorine radicals. Although both the lateral etch and the vertical etch can occur during the RIE process, the nature of the ultrathin flake makes the vertical etch prominent, as shown in Fig. 2(b), where the thin area of the flake was etched away inside the red circle. Therefore, we believe that few-layer β-Ga_2O_3 flake can be obtained by optimizing the RIE-assisted thinning process. AFM images (Figs. 2(c) and 2(d)) of the flakes also confirm that the flake was uniformly thinned by RIE. The as-transferred β-Ga_2O_3 flake consisted of three regions: from the left-top, the heights of the regions were 300, 404, and 527 nm, respectively. AFM image of the flake after RIE-assisted thinning is shown in Fig. 2(d), where a reduction of the width of the flake is clearly evident. To analyze the change in the height by etching, the thicknesses of the three regions that were mentioned above were re-measured, where the heights became 150, 255, and 378 nm, respectively. Since the sapphire substrate was also plasma-etched in addition to the β-Ga_2O_3 flake, the changes in the height include the total etched height of the sapphire and β-Ga_2O_3. The etch rate of the sapphire substrate was estimated to be ~6 nm/min under the above-mentioned conditions, when averaged over 15 min. However, three areas with different heights were maintained, which indicates that the same face is uniformly thinned by RIE. Height profiles of the RIE-thinned β-Ga_2O_3 flake were measured along the scan lines marked in Figs. 2(a) and 2(b), showing that the thinnest flake had a height of ~60 nm. Although the large difference between the lattice constants allows mechanical exfoliation to occur in β-Ga_2O_3, the thickness of the mechanically exfoliated β-Ga_2O_3 is normally over 200 nm because β-Ga_2O_3 is not a van der Waals material. The reduction in width caused by the plasma etch was also confirmed by comparing the

AFM and microscope images, implying that our method can be used to define the channel area because the size and shape of the exfoliated flakes are difficult to be controlled. Edge of the flake was recessed by approximately 1 μm as a result of 15 min etch, which is very fast. It appears that the edge of the flake was readily etched from both the vertical and lateral sides simultaneously, which resulted in a higher etch rate. To obtain the etch rate under various conditions, we used the 100 and 200 W power levels for 5, 10, and 15 min. Figure 2(f) shows the results of each etch depth. At 100 W, the etch depth was negligible. A linear relationship between etch depth and time was observed at 200 W. Based on these results, it can be determined that an etch rate of 16.4 nm/min was obtained using a SF_6 plasma with a flow of 50 sccm at 200 W.

SF_6 gas reacts with β-Ga_2O_3, forming volatile oxygen fluoride compounds (and possibly oxygen) and non-volatile GaF_X, which has a low vapor pressure. Sreenidhi *et al.*[28] etched GaN and obtained an etch rate of ~10.6 nm/min using an SF_6/Ar plasma, reporting that Ar helps to more efficiently remove the non-volatile GaF_X formed during etching; this, in turn, helps to improve the etch rate. Similarly, Basak *et al.*[29] etched GaN using SF_6 and obtained an etch rate of 5.4 to 15.4 nm/min for bias voltages from 250 to 400 V. They concluded that the etching mechanism is the formation of volatile NF_X and non-volatile GaF_X, the removal of which is facilitated by the physical sputtering effects. The etching mechanism of β-Ga_2O_3 is likely similar to the previous reports of GaN etch. SF_6 reacts with the surface of the β-Ga_2O_3 flake and forms the GaF_X. Then, bombardment by positive ions eliminates the GaF_X layer effectively by physical sputtering. Our etch rate is comparable to that with chlorine-based gas (~8 nm/min) where volatile compounds such as $GaCl_X$ form. However, SF_6 has a merit of less toxicity, less corrosiveness, and less compatibility with the silicon manufacturing process.

A top-view SEM image of β-Ga_2O_3 flake etched for 15 min is shown in Fig. 3(a), demonstrating that the surface of the RIE-etched flake was very smooth. Figure 3(b) is a cross-sectional TEM image of an etched β-Ga_2O_3 flake where Pt was deposited to protect the surface of the flake during the focused-ion beam cutting. Less crystallinity was observed at the surface region (~5 nm) between Pt and β-Ga_2O_3, indicating the presence of plasma-induced damage on the surface. A selected area electron diffraction (SAED) pattern is displayed in the inset of Fig. 3(b). Although a dim ring pattern induced by etching damage is observed, other diffraction patterns are evident, which confirms the minimal etching damage as well as the preservation of the crystallinity. We believe that the damage on the surface can be minimized by optimizing the etch conditions. One of the techniques used to analyze the defects is micro-Raman spectroscopy. Although Raman spectroscopy is generally employed to analyze the volumetric properties of the sample, it is also sensitive to the biaxial strain and the defects on the surface. Fig. 3(c) shows the evolution of Raman spectra of the RIE-thinned β-Ga_2O_3. From the top of graph, the Raman spectra normalized with the Si peak are displayed at 5 min intervals for 30 min etch, where the phonon modes are in good agreement with the previous report.[30] The position of the Raman shift and the full width at half maximum of the peaks were both analyzed, implying that there was nominal change, which is consistent with the results of SEM and TEM.

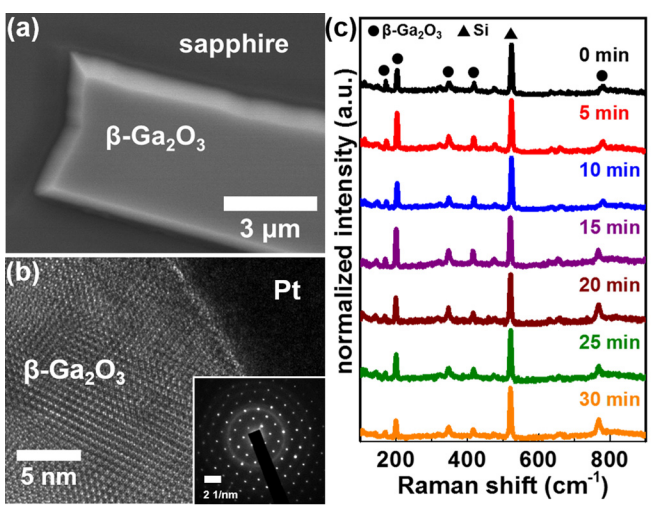

FIG. 3. (a) SEM image of the β-Ga_2O_3 flake etched for 15 min. (b) Cross-sectional TEM image of a plasma-etched β-Ga_2O_3 flake (inset: SAED pattern). (c) Evolution of Raman spectra of β-Ga_2O_3 flake at 5 min intervals for 30 min etch.

To investigate the opto-electronic properties of the plasma-thinned β-Ga_2O_3, we fabricated a photoconductive-structured solar-blind photodetector using an etched β-Ga_2O_3 flake. They were characterized in the dark, and also under illumination at UV-visible wavelengths of 532, 365, and 254 nm by measuring the photocurrents as shown in Fig. 4(a). The linear I-V curve suggests that good Ohmic contacts were formed between the β-Ga_2O_3 flake and the Ti/Au electrode. Bae *et al.*[21] reported that Ti/Au electrodes can form Ohmic contacts with unintentionally doped β-Ga_2O_3. In our experiments, a drastic increase of current, which was higher than results of previous studies, was observed due to the increased number of donor-like defect centers. Higashiwaki *et al.*[2] demonstrated that the RIE treatment could generate a large density of surface defects, such as vacancies, that can act as donors. According to Ping *et al.*,[31] the damage induced by the $SiCl_4$ was beneficial for improving Ohmic contacts on GaN. For the photoresponse of the solar-blind device at different wavelengths, there was no meaningful change between dark condition and 532 nm illumination; however, a noticeable response was observed under 365 and 254 nm UV light. It is expected that β-Ga_2O_3 should have no responsivity above ~290 nm because of its ~4.9 eV bandgap. However, pristine β-Ga_2O_3 flakes showed similar behavior at visible wavelengths, which is attributed to the presence of intrinsic defects including oxygen vacancies.[20] Fig. 4(b) shows the time-dependent photocurrent under illumination at different wavelengths of 254, 365, and 532 nm; each peak was normalized by the dark current. As mentioned above, there was no change at 532 nm, but a change of current was observed at 254 and 365 nm. The photoresponse at 254 nm was higher than that at 365 nm due to the band-to-band excitation. On the other hand, defect-to-band or band-to-defect excitations are the main factor for the photocurrents at 365 nm. For a more detailed analysis, the photocurrent peaks at 254 and 365 nm were fitted using a bi-exponential relaxation equation below (Figs. 4(c) and 4(d))[32–34]

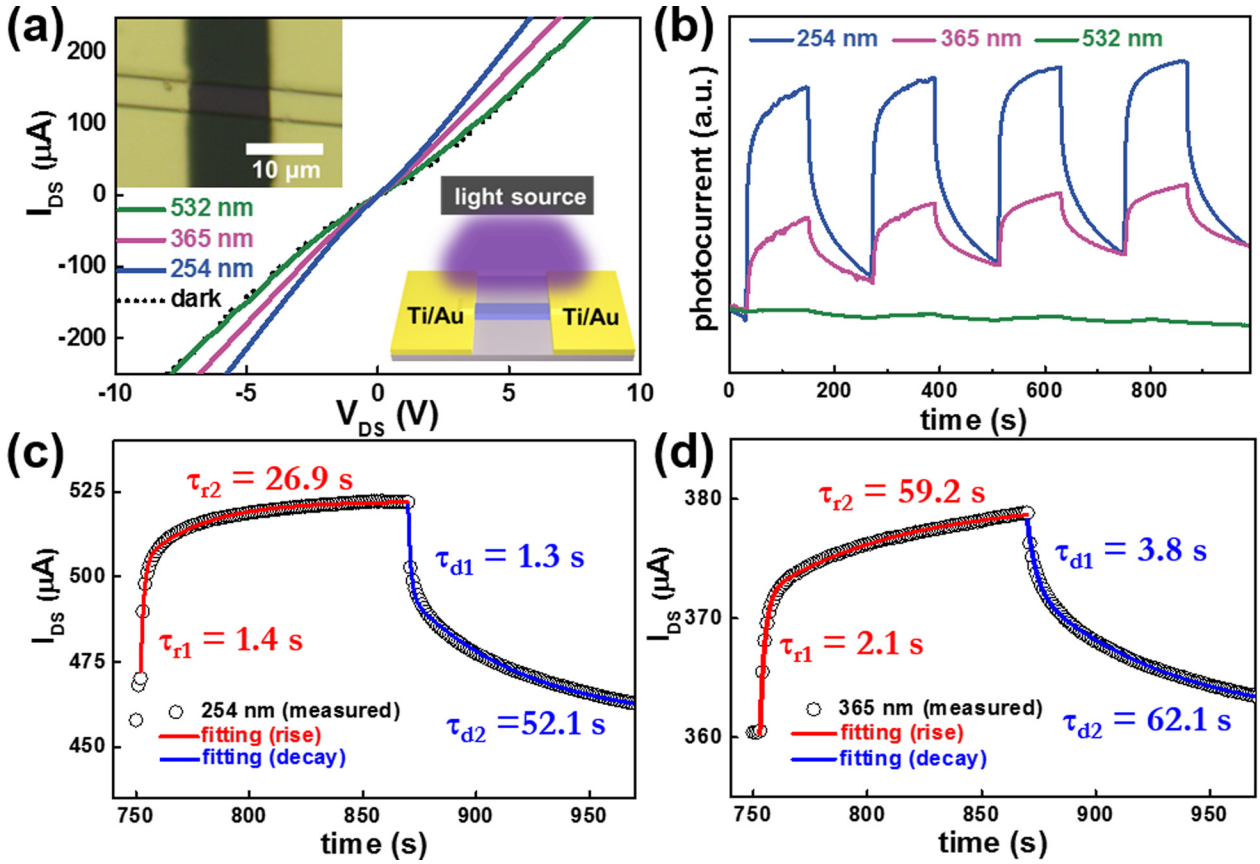

FIG. 4. (a) I-V characteristics under different illumination conditions [inset: optical image of the fabricated device (upper left) and schematic of experimental set-up for light detection (lower right)]. (b) The normalized time-dependent photocurrent under 254, 365, and 532 nm illuminations. Experimental data and curve-fitting of the photocurrent under (c) 254 nm and (d) 365 nm wavelengths.

$$I = I_0 + Ae^{\frac{-t}{\tau_1}} + Be^{\frac{-t}{\tau_2}}.$$

I_0 is the steady-state current, A and B are constants, and t is the time. Both τ_1 and τ_2 are relaxation time constants, and we defined τ_1 and τ_2 as the fast and slow response time constants, respectively. τ_r and τ_d are constants in the rise and decay regions, respectively. Since the response and decay time constants are related to the defective sites, we compared them by using the un-etched and etched flakes and conclude that the results are comparable,[20] indicating that the plasma-assisted thinning of the exfoliated β-Ga_2O_3 flake did not degrade its opto-electronic properties.

In summary, mechanically exfoliated β-Ga_2O_3 flakes were thinned by using RIE with SF_6, demonstrating a high etch rate of 16.4 nm/min with good uniformity on flakes thinned to ~60 nm. Volatile oxygen fluoride compounds and non-volatile etch products such as GaF_X were removed by ion-assistance, producing smooth morphology. A reduction of width as well as height of the flakes was observed as a result of the plasma etching. Optical, structural, and morphological properties of the plasma-thinned β-Ga_2O_3 flakes were characterized. Solar-blind photodetector devices based on the plasma-thinned β-Ga_2O_3 flakes showed that the opto-electronic properties were preserved through the thinning process. Our RIE-based thinning method proposes a scalable and industry-compatible way to control the thickness of the exfoliated 2D flakes for the implementation of 2D material-based nanodevices.

The research at Korea University was supported by the Korea Institute of Energy Technology Evaluation and Planning (KETEP) and the Ministry of Trade, Industry & Energy (MOTIE) of the Republic of Korea (No. 20163010012140 and No. 20153030012110) and National Research Foundation of Korea (2016M3D1A1952967) funded by the Ministry of Science, ICT and Future Planning of Korea.

[1]M. Orita, H. Ohta, M. Hirano, and H. Hosono, Appl. Phys. Lett. **77**, 4166 (2000).
[2]M. Higashiwaki, K. Sasaki, A. Kuramata, T. Masui, and S. Yamakoshi, Appl. Phys. Lett. **100**, 013504 (2012).
[3]B. J. Baliga, IEEE Electron. Dev. Lett. **10**, 455 (1989).
[4]R. Zou, Z. Zhang, Q. Liu, J. Hu, L. Sang, M. Liao, and W. Zhang, Small **10**, 1848 (2014).
[5]C. Hsu and Y. Lu, Nanoscale **4**, 5710 (2012).
[6]Y. Li, T. Tokizono, M. Liao, M. Zhong, Y. Koide, I. Yamada, and J. J. Delaunay, Adv. Funct. Mater. **20**, 3972 (2010).
[7]Z. Galazka, R. Uecker, K. Irmscher, M. Albrecht, D. Klimm, M. Pietsch, M. Brützam, R. Bertram, S. Ganschow, and R. Fornari, Cryst. Res. Technol. **45**, 1229 (2010).
[8]K. Irmscher, Z. Galazka, M. Pietsch, R. Uecker, and R. Fornari, J. Appl. Phys. **110**, 063720 (2011).
[9]H. Aida, K. Nishiguchi, H. Takeda, N. Aota, K. Sunakawa, and Y. Yaguchi, Jpn. J. Appl. Phys., Part 1 **47**, 8506 (2008).
[10]T. Oishi, Y. Koga, K. Harada, and M. Kasu, Appl. Phys. Express **8**, 031101 (2015).
[11]Y. Tomm, J. Ko, A. Yoshikawa, and T. Fukuda, Sol. Energy Mater. Sol. Cells **66**, 369 (2001).
[12]H. G. Kim and W. T. Kim, J. Appl. Phys. **62**, 2000 (1987).
[13]D. Splith, S. Müller, F. Schmidt, H. Von Wenckstern, J. J. van Rensburg, W. E. Meyer, and M. Grundmann, Phys. Status Solidi A **211**, 40 (2014).

[14]K. Sasaki, A. Kuramata, T. Masui, E. G. Víllora, K. Shimamura, and S. Yamakoshi, Appl. Phys. Express **5**, 035502 (2012).
[15]S. Lee, K. Kaneko, and S. Fujita, Jpn. J. Appl. Phys. **55**, 1202B8 (2016).
[16]W. S. Hwang, A. Verma, H. Peelaers, V. Protasenko, S. Rouvimov, H. Xing, A. Seabaugh, W. Haensch, C. V. de Walle, and Z. Galazka, Appl. Phys. Lett. **104**, 203111 (2014).
[17]J. Kim, S. Oh, M. A. Mastro, and J. Kim, Phys. Chem. Chem. Phys. **18**, 15760 (2016).
[18]S. Ahn, F. Ren, J. Kim, S. Oh, J. Kim, M. A. Mastro, and S. Pearton, Appl. Phys. Lett. **109**, 062102 (2016).
[19]R. Mitdank, S. Dusari, C. Bülow, M. Albrecht, Z. Galazka, and S. Fischer, Phys. Status Solidi A **211**, 543 (2014).
[20]S. Oh, J. Kim, F. Ren, S. J. Pearton, and J. Kim, J. Mater. Chem. C. **4**(39), 9245 (2016).
[21]J. Bae, H. Kim, and J. Kim, ECS J. Solid State Sci. Technol. **6**, Q3045 (2017).
[22]K. S. Novoselov, A. K. Geim, S. Morozov, D. Jiang, M. Katsnelson, I. Grigorieva, S. Dubonos, and A. Firsov, Nature **438**, 197 (2005).
[23]G. Lee, J. Lee, G. Lee, and J. Kim, J. Mater. Chem. C **4**, 6234 (2016).
[24]S. Ohira and N. Arai, Phys. Status Solidi C **5**(9), 3116 (2008).
[25]T. Oshima, T. Okuno, N. Arai, Y. Kobayashi, and S. Fujita, Jpn. J. Appl. Phys., Part 1 **48**, 040208 (2009).
[26]J. E. Hogan, S. W. Kaun, E. Ahmadi, Y. Oshima, and J. S. Speck, Semicond. Sci. Technol. **31**, 065006 (2016).
[27]H. Manasevit and F. Morritz, J. Electrochem. Soc. **114**, 204 (1967).
[28]T. Sreenidhi, N. DasGupta, and K. Baskar, presented at the International Workshop on Physics of Semiconductor Devices, IWPSD 2007.
[29]D. Basak, M. Verdu, M. Montojo, M. Sanchez-Garcia, F. Sanchez, E. Munoz, and E. Calleja, Semicond. Sci. Technol. **12**, 1654 (1997).
[30]C. Kranert, C. Sturm, R. Schmidt-Grund, and M. Grundmann, Sci. Rep. **6**, 35964 (2016).
[31]A. Ping, Q. Chen, J. Yang, M. A. Khan, and I. Adesida, J. Electron. Mater. **27**, 261 (1998).
[32]D. Guo, Z. Wu, P. Li, Y. An, H. Liu, X. Guo, H. Yan, G. Wang, C. Sun, and L. Li, Opt. Mater. Express **4**, 1067 (2014).
[33]N. Liu, G. Fang, W. Zeng, H. Zhou, F. Cheng, Q. Zheng, L. Yuan, X. Zou, and X. Zhao, ACS Appl. Mater. Interfaces **2**, 1973 (2010).
[34]D. Guo, Z. Wu, Y. An, X. Guo, X. Chu, C. Sun, L. Li, P. Li, and W. Tang, Appl. Phys. Lett. **105**, 023507 (2014).